MEMS-Based Tunable Metamaterials

Subjects: Optics | Engineering, Electrical & Electronic

Contributor: Yu-Sheng Lin

Micro-electro-mechanical systems (MEMS) is a well-known technology that mechanically reconfigures the metamaterial unit cells.

metamaterials metasurfaces nanophotonics

1. Introduction

Metamaterial, an artificial periodic micro/nanostructure used to manipulate the propagation of electromagnetic (EM) waves, has drawn a great deal of attention due to its unique electromagnetic properties [1][2][3]. By properly engineering the geometrical dimensions and material compositions of their subwavelength periodic unit cells, the permittivity and permeability of metamaterials can be manually controlled. Owing to that, metamaterials are widely studied in cloaking devices, energy harvesting, medical imaging, negative refraction index, and so on [4][5][6]. The operating wavelength range of metamaterials can be spanned in the entire EM spectrum by physically scaling the geometry, starting from visible light [7][8][9][10] to infrared (IR) [11][12][13][14], terahertz (THz) [15][16][17][18][19][20], and microwaves [21][22][23][24]. Many metamaterial-based optical devices have been demonstrated to have powerful performances [25][26][27][28]. However, these rigid devices cannot be actively tuned once fabricated. The controllable metamaterials help to improve flexibility by using an external stimulus. To satisfy this requirement, there are many techniques proposed for tuning mechanisms, including micro-electro-mechanical systems (MEMS) technology [29], thermal annealing [30], phase-transition materials [31][32][33], two-dimensional material [34][35][36], laser pumping [37], and liquid crystals [38]. Among these, MEMS technology is a promising technique for actively tunable metamaterial due to its ability to directly modify the metamaterial unit cells. Moreover, MEMS tuning methods can provide an ideal platform for metamaterial, which is not limited by the nonlinear characteristic of natural materials and exhibits a large tuning range of resonant frequency [39][40].

In recent years, active MEMS-based tunable metamaterial has become a hotspot in optoelectronics research as it provides the possibility to manually manipulate electromagnetic waves. By utilizing MEMS technologies, the metamaterial can be directly reconfigured and achieve wide applicability. **Figure 1** illustrates the development of MEMS-based metamaterials in the last ten years, which indicates the diversification growth of MEMS tuning methods. In 2011, the geometric dimension of metamaterial was horizontally modified by exploiting the MEMS comb-drive actuator platform. Owing to that, Zhu et al. proposed a THz micro-ring metamaterial to achieve a large tuning range and the change of polarization-dependent states [41]. In 2012, by changing the configuration to the Maltese-cross pattern, they demonstrated a THz metamaterial with anisotropy tunable from positive to negative values [42], which showed the various applications of a stable MEMS-based metamaterial platform. In 2013, Liu et

al. exhibited a mechanically actuated metamaterial capable of high-speed intensity modulation of IR radiation in a reflection configuration [43]. In the same year, Lin et al. demonstrated continuously tunable stress-induced curved cantilevers to form double split-ring resonators (DSRR) in a three-dimensional configuration to provide a higher tuning range of resonant frequency [44]. Since metamaterial can be highly integrated with MEMS technology, it is possible for metamaterial to be implanted in the actuator design. In 2015, Pitchappa et al. proposed interpixelated MEMS metamaterials for the realization of excellent switching performance [45]. Such switchable characteristics enable the realization of programmable metamaterials with higher intelligence. Along with the development of digital metamaterial, they demonstrated the microcantilevers integrated into a single unit cell for independent control of the orthogonal THz polarization response in 2016 [46]. Since then, the reconfigurable characteristic of MEMS-based metamaterial has been desired for its significant application, such as logic operation and sensing. In 2017, Liu et al. proposed a reconfigurable room temperature metamaterial IR emitter, whose displaying pixel is composed of MEMS metamaterial [47]. While the scope of application in MEMS-based metamaterial is gradually enlarged, Zhao et al. presented a tunable cantilever metasurface array to be used as a CMOS-compatible tunable quarter-wave plate in 2018 [48]. In 2019, Xu et al. demonstrated a stretchable THz parabolic-shaped metamaterial based on polydimethylsiloxane (PDMS) substrate and showed that flexible substrate can be exploited to mechanically control the metamaterial with high efficiency [49]. Mo et al. proposed a face-to-face chevron-shaped metamaterial to achieve vertical and horizontal tunings in 2020 [50]. In 2021, to enlarge the incident angle of received light and enhance the switching performance, Xu et al. proposed an actively tunable optical metadevice by integrating self-assembly electrothermal actuator and magnetic metamaterial [51]. Such a magnetic actuating method provides an ideal MEMS-based metamaterial platform with a large tilt angle and displacement. These milestone developments of actively MEMS-based metamaterial contribute a lot to the widespread applications of tunable optical devices, such as logic operation, sensing, energy harvest, display, and so on [52][53][54][55][56][57].

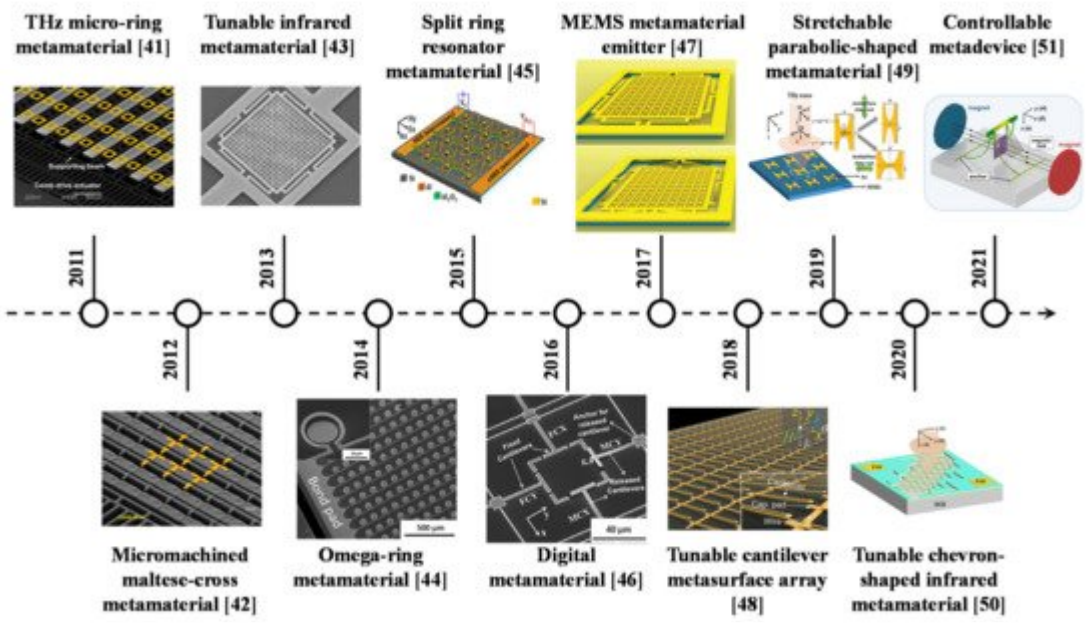

Figure 1. The development of MEMS-based tunable metamaterial in the last ten years.

2. MEMS-Based Metamaterial Emerging

The typical MEMS-based metamaterials exploit several actuating methods, including electrostatic actuators (ESAs), electrothermal actuators (ETAs), and electromagnetic actuators (EMAs). The stretchable MEMS-based metamaterials are realized by simply using a flexible substrate.

2.1. ETA-Based Metamaterial

2.1.1. Vertical Tuning Methods

The geometrical dimension is a key factor to determine the EM wave characteristics of a metamaterial. Since the first ETA-based reconfigurable THz metamaterials were demonstrated by using a thermal stimulus, as shown in **Figure 2**a, ETA vertical tuning methods have been widely applied in metamaterials for large physical displacement [58]. Such methods are mainly based on microcantilevers to support the continuous tuning states of lifting up and lifting down. The microcantilevers are required to comprise a multi-layer with a large difference in thermal expansion coefficients between various materials. Through the heating process, the various thermal expansions provide tensile and compressive residual stress between different layers. Thus, ETAs can be deformed upwards by an initial strain force to perform a prestressed state. **Figure 2**b shows the electrical split-ring resonators (eSRR) based on metamaterial microarray [59]. With the increased external temperature from 77 K to 400 K, the resonant frequency can be continuously red-shifted 80 GHz for the advanced manipulation of THz waves. Meanwhile, ETAs are widely reported to modify the vertical gap between different metamaterial layers, as shown in **Figure 2**c,d [60] [61]. In such designs, strong coupling resonances are induced between vertical layers. Thus, the vertical displacement of ETA is exploited to control the electromagnetic properties of metamaterials.

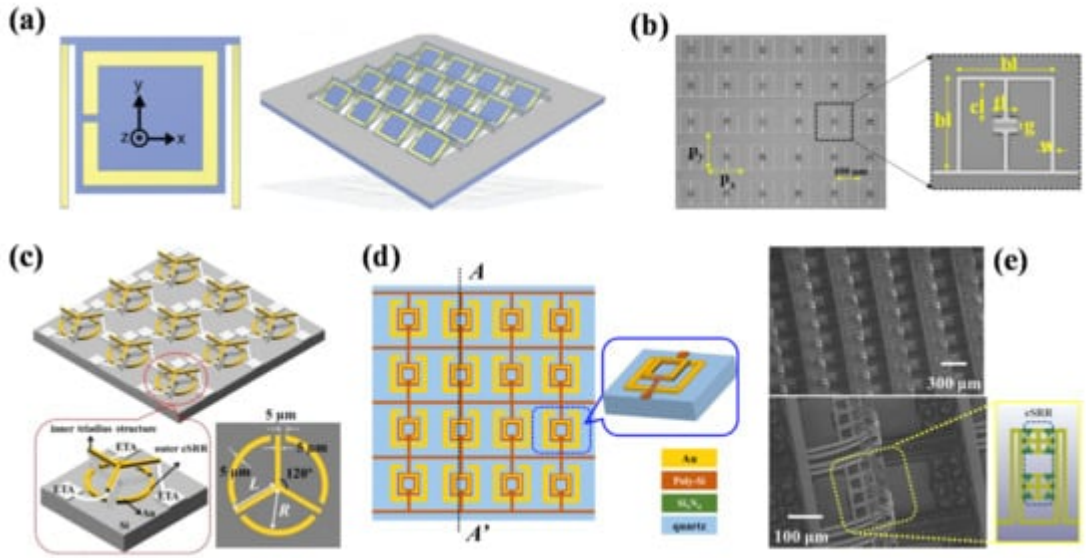

Figure 2. ETA-based vertical tuning methods of metamaterials: (**a**) schematic of thermally tunable split-ring resonators (SRR) based on the pre-stressed metamaterial [58]; (**b**) optical microscopy image of the eSRR based on metamaterial microarray [59]; (**c**,**d**) schematic of MEMS-based tunable THz metamaterial and unit cell by using ETA

vertical tuning platforms [60][61]; (**e**) scanning electron microscope (SEM) images of eSRR–WCM array and unit cell [62].

While the external heating process is incompatible with CMOS-based devices, the voltage-controllable ETA tuning methods are desired to improve integration. Thus, resistance heat is exploited to increase the temperature of ETA. By applying voltage on the ETA-based metamaterial, a large amount of resistance heat can be induced by current flow to directly control the deformed height of ETA. Moreover, such voltage-controllable methods are reconfigurable. **Figure 2**e shows a winding-shaped cantilever metamaterial (WCM) array integrated with eSRR under a pre-deformed state [62]. The metamaterial layer is tailored to conduct the resistance heat—which can be induced—and the deformed height of ETA and then actively become tuned by applying a DC voltage. By modifying the driving voltage, the propagation of EM waves can be manually controlled to achieve electric-optical modulation. Such an ETA-based vertical tuning method provides a cost-effective platform to design metamaterials with a large tuning range.

2.1.2. Horizontal Tuning Methods

ETAs can further provide horizontal displacement for tunable metamaterial by using a chevron beam and a hot-cold arm. The chevron beam ETA is a typical design in MEMS actuators. By applying a voltage on the ends of ETAs to increase the temperature, the center shuttle of actuators can be moved due to the thermal expansion on both sides of the chevron beams. **Figure 3**a indicates a tunable metamaterial based on a two-cut SRR unit cell and the tuning mechanism [63]. While the center shuttle of the chevron beam actuator generates a displacement, the slabs move towards the cuts of the two-cut SRR, which achieves a continuous tuning method for the metamaterial by changing the gap between slabs and SRR. A reconfigurable THz metamaterial is obtained from the embedment of a chevron beam ETA as shown in **Figure 3**b [64]. By applying the appropriate actuation voltage on ETAs, the enhanced bandwidth tunability at two different resonances can be accomplished.

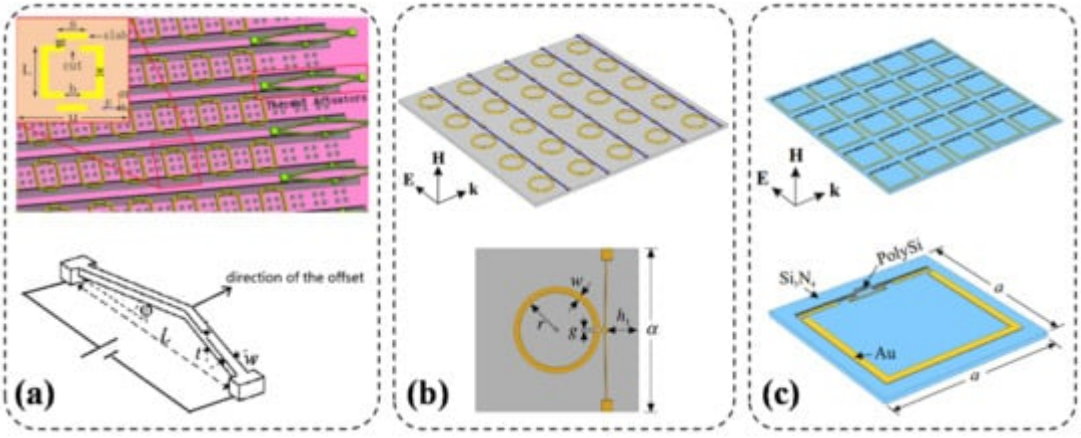

Figure 3. ETA-based horizontal tuning methods of metamaterial: (**a**) schematic of the tunable metamaterials and the two-cut SRR unit cell [63]; (**b**) schematic of tunable metamaterial and the unit cell using the chevron beam ETA [64]; (**c**) schematic of two independent ETA, SRR, and unit cell [65].

The cold-hot-arm based ETAs can achieve the increment of power consumption efficiency and larger curvature compared with the design of chevron beam ETA. In this method, by applying an external voltage, the electric current flows along the hot arms to generate resistive heating and thermal expansion. While the cold arms are not connected to the electric flowing loop and remain at low temperature, a large deflection can be induced owing to the thermal expansion difference between hot and cold arms. **Figure 3**c shows a tunable metamaterial based on the combination of two-hot-arm ETAs with an SRR [65]. The tuning methods provide the mu-negative behavior via a low voltage. These results prove that the horizontal ETA is a promising method for tunable metamaterial to be used in low voltage applications.

2.2. ESA-Based Metamaterial

2.2.1. Vertical Tuning Methods

ESA is a commercial and mature MEMS actuating method, which induces an electrostatic motion by driving an electrical input. To enable the vertical displacement, the electrical potential difference is usually induced between different conductive layers, i.e., a metallic layer and a semiconductor substrate. **Figure 4**a shows a tunable THz filter based on a DSRR structure released from a silicon substrate [66]. By applying different DC bias voltages between metallic SRR layers and silicon substrates, the bending degree of micro-cantilever can be continuously changed to realize a large frequency tuning range and high quality (Q)-factor. Meanwhile, the released SRR cantilevers will be snapped down to silicon substrate with the DC bias higher than the pull-in voltage. Liu et al. designed and experimentally demonstrated ultrathin tunable THz absorbers based on MEMS-based metamaterial, as shown in **Figure 4**b [67]. These were composed of a metallic ground plane, a silicon nitride spacer, and a matrix of meta-atoms from bottom to top. The metamaterial membranes were suspended above the silicon nitride layer by a distance, which was adjustable with different driving electrostatic forces. By applying a voltage, the absolute absorption modulation range measured at the initial resonance could reach 65%. In **Figure 4**c, a MEMS-based metasurface is demonstrated for active control of the Fano-resonances [68]. Two SRRs can be independently and sequentially actuated by applying the voltages. With multiple inputs and outputs to represent on and off digital states, such designs are suitable for logic operations at the THz frequencies. Several planar arrays of eSRR with movable stress curved beams are proposed as shown in **Figure 4**d,e, which are actuated out-of-plane by electrostatic force [69][70]. **Figure 4**f shows a tunable THz filter and a modulator based on ESA-metamaterial [71]. A radio frequency-MEMS (RF-MEMS) capacitor is embedded in the center of each SRR unit cell to tune the electromagnetic resonant frequency, while the modulation speed can reach 2 kHz. **Figure 4**g indicates an active MEMS metamaterial for the THz bandwidth control, which consists of an array of sixteen cantilever resonators with gradually varying release lengths [72]. By electrostatically controlling the out-of-plane height of the released micro-cantilever-based resonators, the full width half maximum (FWHM) resonance bandwidth of the MEMS metamaterial can be actively switched to 90 GHz. With a supercell composed of several cantilevers, the switching range can be further improved, as shown in **Figure 4**h [73]. Each metamaterial unit cell consists of eight cantilevers placed at the corner of an octagon ring to achieve a large tuning range of 0.37 THz. **Figure 4**i shows a structurally reconfigurable metamaterial for active switching of near-field coupling in conductively coupled, orthogonally twisted SRRs [74]. SRRs structures are precisely tailored to excite the classical analogue of electromagnetically induced transparency

(EIT) by the strong conductive coupling. In **Figure 4**j,k, the ESA-based tunable THz metamaterials using three-dimensional eSRR arrays are proposed to realize polarization-sensitivity and flow tuning capability, respectively [75] [76]. It can be clearly observed that the ESA-based vertical tuning method provides a mature platform for metamaterial and opens an avenue for more potential applications, such as logic operation, EM wave modulation, flowing sensing, and so on [77][78][79].

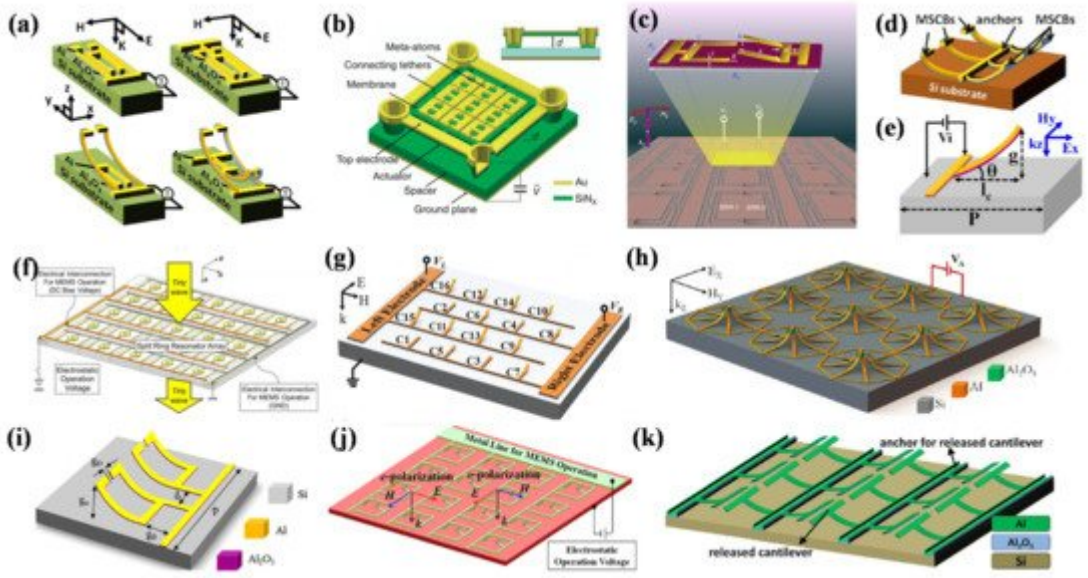

Figure 4. ESA-based vertical tuning methods of metamaterial: (**a**) schematic of DSRR with single-side and double-side ESA structure under unreleased and released state, respectively [66]; (**b**) schematic of the unit cell of the THz absorber [67]—the vertical distance between the meta-atoms and the ground plane can be tuned electrostatically; (**c**) colored SEM image of the MEMS Fano metasurface [68]—the periodic unit cell comprises of two SRRs; (**d**) schematic of electric split-ring resonators with movable stress-curved beams (eSRR-MSCBs) after microstructures are released [69]; (**e**) schematic of an upward bent microcantilever as metamaterial unit cell [70]; (**f**) MEMS reconfigurable SRR design array of the unit cell [71]; (**g**) schematics of a bandwidth tunable MEMS metamaterial supercell formed by a 4 × 4 array of microcantilever resonators with varying fixed and released lengths [72]; (**h**) schematics of the proposed uniaxially isotropic MEMS metamaterial with eight released cantilevers in an octagon ring [73]; (**i**) schematics of the conductively coupled MEMS metamaterial [74]; (**j**) schematics of the chained eSRR array with a metal line connecting the eSRRs for MEMS operation [75]; (**k**) schematic of the mirrorlike T-shape metamaterial (MTM) device after release [76].

2.2.2. Horizontal Tuning Methods

Comb driver is a typical design of ESA that is suitable to horizontally modify the geometry of metamaterial. Comb drivers are composed of fixed combs and movable combs. By applying a voltage potential difference on combs, an electrostatic force can be generated to drive a movable comb to approach a fixed comb. Moreover, the comb driver can suitably provide a tunable platform for the whole metamaterial array to achieve better uniformity of deformation in each unit cell. **Figure 5**a shows reconfigurable asymmetric split-ring resonators (ASRRs) metamaterial [80]. Two identical electrostatic comb-drive actuators are employed on both sides for a mechanically balanced translation of

the supporting frame, which can realize a horizontal displacement of 20 μm. Similarly, switchable ESA-based metamaterials are demonstrated by using fixed SRR and moveable SRR as shown in **Figure 5**b,c [81][82]. By reshaping the micromachined metamaterial unit cells, the surface resonance of the metamaterial is manually controlled. **Figure 5**d indicates a tunable metamaterial consisting of two SRR array layers [83]. The top SRR layer is on a movable silicon frame that can be actuated by a comb-drive actuator while the bottom SRR layer is fixed on a SiNx thin-film. By applying voltage on the comb driver, a continuous lateral shifting between the coupled resonators can be induced to 20 μm. A MEMS integrated device is proposed by using EIT metamaterial, as shown in **Figure 5**e [84]. The comb driver design is composed of a fixed beam and a movable beam based on a silicon on insulator (SOI) wafer. In **Figure 5**f, a reconfigurable metasurface is proposed to achieve both the polarization conversion and the polarization rotation in the THz frequency range by using the comb driver [85]. In the IR wavelength range, ESA-based metamaterials are also reported to realize active modulation of the polarization state, as shown in **Figure 5**g [86]. In **Figure 5**h–j, Xu et al. propose several SRR patterns integrated with the comb driver platform to be operated at different frequencies, which can be applied in many fields, such as tunable filters, frequency-selective detectors, polarization switches, high-efficient environmental sensors, and more [87][88][89]. From these literature reports, the ESA-based platform shows great applicability for the horizontal tunable metamaterial. The comb driver provides more mature tuning methods compared with other MEMS tuning mechanisms. The geometry of integrated metamaterial is rapidly reduced, which means the MEMS-based metamaterial can be gradually operated from THz and IR, as well as visible spectra [90].

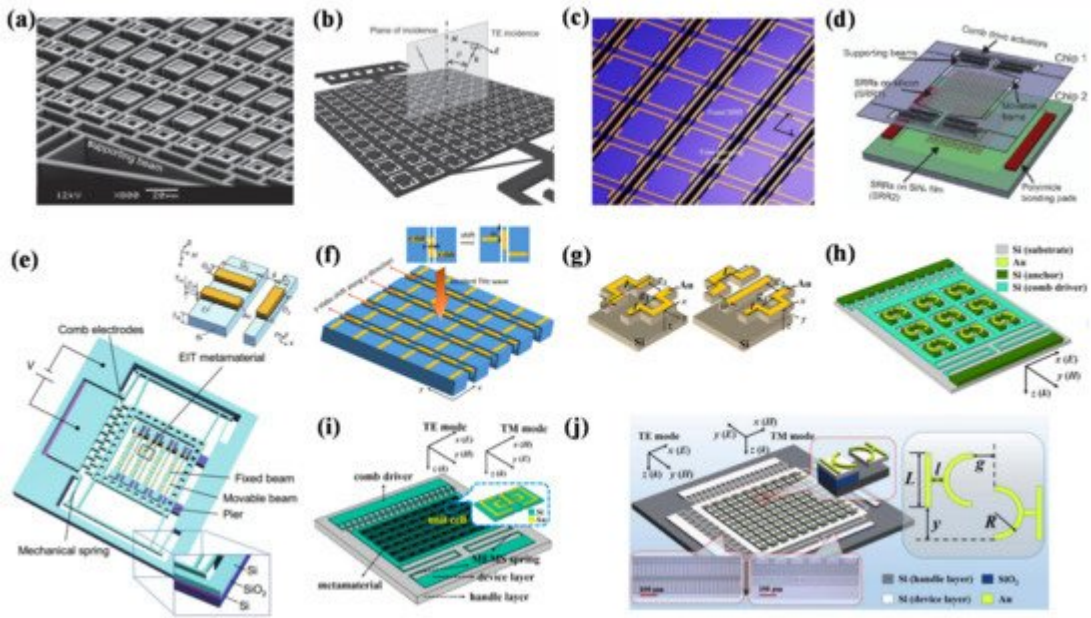

Figure 5. ESA-based horizontal tuning methods of metamaterial: (**a**) SEM images of the reconfigurable ASRRs metamaterial [80]; (**b**) schematic of the switchable magnetic metamaterial consisting of two semi-square split rings separated by a gap [81]; (**c**) schematics of the micromachined metamaterial with the element consisting of a two-cut SRR and two free-hanging slabs [82]; (**d**) schematic of the tunable metamaterials, including broadside-coupled SRRs (BC-SRRs) [83]; (**e**) schematic of the MEMS integrated device—unit cell of the EIT metamaterial consists of a cut wire and a wire pair [84]; (**f**) schematics of the tunable metasurface for the polarization conversion and the

polarization rotation [85]; (**g**) schematics of polarization-sensitive IR metamaterials (PSIMs) [86]; (**h**–**j**) schematic of a tuning eSRR array by using comb drive horizontal tuning platforms [87][88][89].

2.3. EMA-Based Metamaterial

A change in the external magnetic field can cause a motion in EMA, which is composed of magnetic materials. **Figure 6**a shows a Ferrite-based magnetically tunable left-handed metamaterial by introducing yttrium iron garnet rods into SRRs/wires periodic array [91]. Thus, by using external DC applied magnetic fields, the left-handed passband of the metamaterial can be continuously and reversibly adjusted. **Figure 6**b indicates a low-voltage three-axis EMA-based micro-mirror to support optical devices [92]. The frame is connected to the robust torsion bar and lifting bar structure formed by bulk silicon to perform greater operating stability. A flexible and controllable metadevice is proposed by using self-assembly MEMS-based ESA, as shown in **Figure 6**c [51]. While the center metamaterial plate is released by the supporting arm, it can be actuated and rotated by a magnetic force to manipulate the incident electromagnetic response by driving the external electromagnetic field. **Figure 6**d shows a tunable THz metamaterial employing magnetically actuated cantilevers [93]. By coating a magnetic material on the cantilever surface, the released eSRR array can be actuated and the resonant frequency of the structures can be modified. These results indicate that the large displacement and rotation angle of EMA tuning methods provide a great possibility for metamaterial to receive light from a wide incident angle, which can greatly improve the sensitivity of metamaterial.

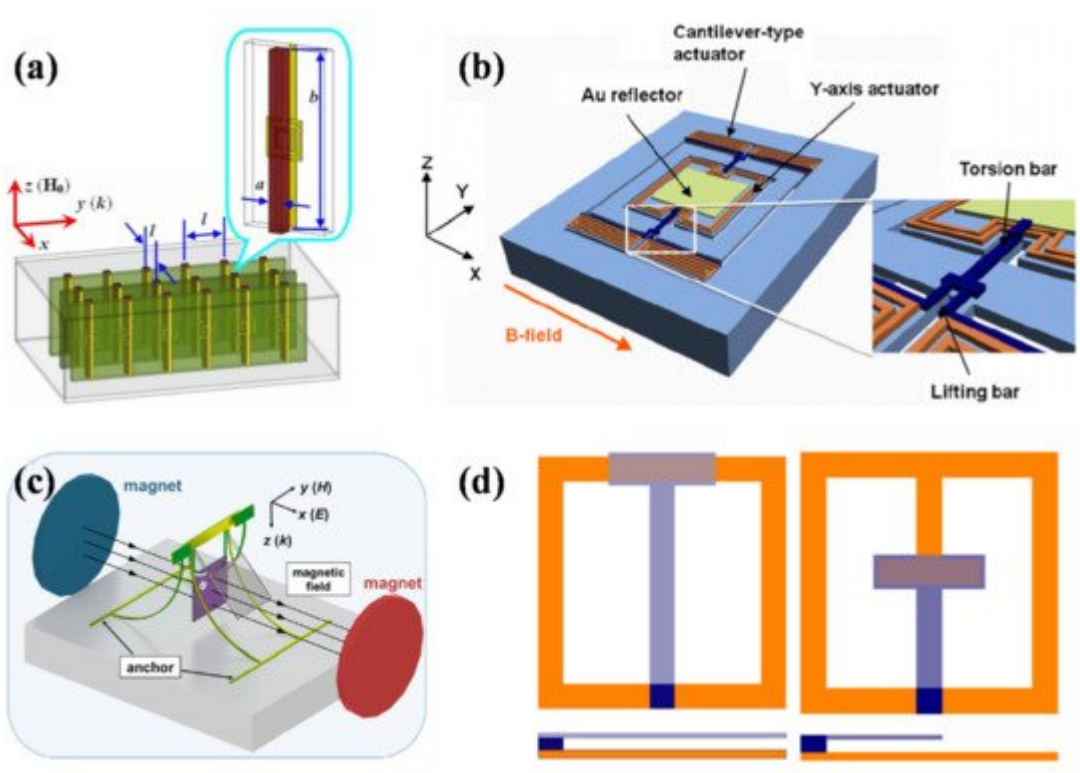

Figure 6. EMA-based tuning methods of metamaterial: (**a**) schematic of the magnetically tunable left-handed metamaterial (LHM) composed of SRRs/wires array and introducing yttrium iron garnet (YIG) rods in rectangular waveguide [91]; (**b**) schematic of the three-axis EMA-based micromirror for fine alignment among optical devices

[92]; (**c**) schematic of active out-of-plane metadevice by driving a magnetic field [51]; (**d**) schematics of an eSRR modified to incorporate a parallel plate capacitor with a flexing cantilever [93].

2.4. Flexible Substrate-Based Metamaterial

In addition to the conventional MEMS actuating mechanisms, the tuning optical characteristic of metamaterial can be realized by using stretchable and flexible substrates, such as PDMS, polyimide, and polyethylene terephthalate (PET) [94][95][96]. It is a simpler mechanical method to provide a large tuning range of resonant frequency. **Figure 7**a shows a THz metamaterial comprising a planar array of I-shaped resonators on a highly elastic PDMS substrate [97]. While such resonators are sensitive to mechanical stretching, the stretching range of metamaterial is over 8% to keep good repeatability over several stretching–relaxing cycles. Zhang et al. demonstrated a mechanically stretchable and tunable metamaterial absorber composed of a dielectric resonator stacked on a conductive rubber, illustrated in **Figure 7**b [98]. By applying different stretching strains to change the elementary cells' periodicity, the operation frequency of the metamaterial absorber is blue-shifted in the microwave spectrum range. A three-layered stretchable metamaterial absorber by using liquid metal and PDMS is proposed in **Figure 7**c [99]. The resonant frequency of the device can be increased from 18.50 GHz to 18.65 GHz, with a stretching length of 1.2 cm, which is suitable to be used as a wireless strain sensor. **Figure 7**d shows a plasmonic antenna-based metasurface on the stretched PDMS [100]. By precisely positioning the Au nanorods, the optical phase is varied over the individual component by a certain amount. Furthermore, the position-dependent phase discontinuity can be further tuned by stretching the metamaterial geometry for reconfigurable flat optics application. **Figure 7**e indicates a stretchable THz parabolic-shaped metamaterial (PSM) to perform logic operations [49]. By stretching the PSM width and length, single-/dual-band switching and polarization switching characteristics can be realized for programmable metamaterials. A tunable perfect absorber with a ring-shaped (PA-RS) and a cross-shaped (PA-CS) on PDMS substrate is proposed in **Figure 7**f [101]. Stretching devices into different directions allows them to exhibit ultra-narrowband, polarization-dependent/independent, and switchable characterizations in the IR wavelength range. The typical advantages of such flexible substrate-based metamaterials are their flexibility and cost-effectiveness, which makes them potentially useful in wearable devices and a variety of sensor fields [102][103].

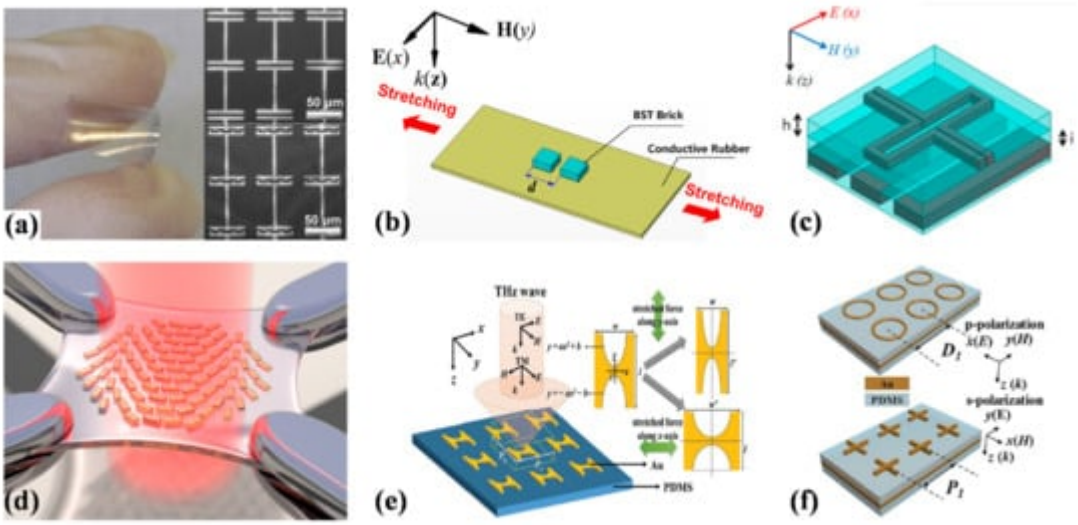

Figure 7. Flexible substrate-based metamaterial: (**a**) photograph and optical micrograph of I-shaped flexible metamaterial design [97]; (**b**) schematic of stretchable dielectric metamaterial absorber [98]; (**c**) schematics of stretchable metamaterial absorber by using liquid metal as the conductor and PDMS as the substrate [99]; (**d**) schematic of a gold nano-rod metasurface array on stretched PDMS [100]; (**e**) schematic of the PSM device operated by applying a stretching force along the x- and *y*-axis directions [49]; (**f**) schematics of stretchable perfect absorber with ring-shaped (PA-RS) and cross-shaped (PA-CS) structures [101].

References

1. Smith, D.R.; Pendry, J.B.; Wiltshire, M.C.K. Metamaterials and negative refractive index. Science 2004, 305, 788–792.
2. Chen, H.T.; Padilla, W.J.; Zide, J.M.; Gossard, A.C.; Taylor, A.J.; Averitt, R.D. Active terahertz metamaterial devices. Nature 2006, 444, 597–600.
3. Schurig, D.; Mock, J.J.; Justice, B.J.; Cummer, S.A.; Pendry, J.B.; Starr, A.F.; Smith, D.R. Metamaterial electromagnetic cloak at microwave frequencies. Science 2006, 314, 977–980.
4. Cui, Y.; Fung, K.H.; Xu, J.; Ma, H.; Jin, Y.; He, S.; Fang, N.X. Ultrabroadband light absorption by a sawtooth anisotropic metamaterial slab. Nano Lett. 2012, 12, 1443–1447.
5. Fu, K.; Zhao, Z.; Jin, L. Programmable granular metamaterials for reusable energy absorption. Adv. Funct. Mater. 2019, 29, 1901258.
6. Le, D.H.; Lim, S. Four-mode programmable metamaterial using ternary foldable origami. ACS Appl. Mater. Interfaces 2019, 11, 28554–28561.
7. Li, W.; Guler, U.; Kinsey, N.; Naik, G.V.; Boltasseva, A.; Guan, J.; Shalaev, V.M.; Kildishev, A.V. Refractory plasmonics with titanium nitride: Broadband metamaterial absorber. Adv. Mater. 2014, 26, 7959–7965.
8. Ma, H.; Song, K.; Zhou, L.; Zhao, X. A naked eye refractive index sensor with a visible multiple peak metamaterial absorber. Sensors 2015, 15, 7454–7461.
9. Ni, X.J.; Wong, Z.J.; Mrejen, M.; Wang, Y.; Zhang, X. An ultrathin invisibility skin cloak for visible light. Science 2015, 349, 1310–1314.
10. Esposito, M.; Tasco, V.; Todisco, F.; Cuscuna, M.; Benedetti, A.; Scuderi, M.; Nicotra, G.; Passaseo, A. Programmable extreme chirality in the visible by helix-shaped metamaterial platform. Nano Lett. 2016, 16, 5823–5828.
11. Hossain, M.M.; Jia, B.; Gu, M. A metamaterial emitter for highly efficient radiative cooling. Adv. Opt. Mater. 2015, 3, 1047–1051.

12. Su, Z.; Yin, J.; Zhao, X. Soft and broadband infrared metamaterial absorber based on gold nanorod/liquid crystal hybrid with tunable total absorption. Sci. Rep. 2015, 5, 16698.
13. Dao, T.D.; Ishii, S.; Yokoyama, T.; Sawada, T.; Sugavaneshwar, R.P.; Chen, K.; Wada, Y.; Nabatame, T.; Nagao, T. Hole array perfect absorbers for spectrally selective midwavelength infrared pyroelectric detectors. ACS Photonics 2016, 3, 1271–1278.
14. Kim, J.; Han, K.; Hahn, J.W. Selective dual-band metamaterial perfect absorber for infrared stealth technology. Sci. Rep. 2017, 7, 6740.
15. Cong, L.; Xu, N.; Gu, J.; Singh, R.; Han, J.; Zhang, W. Highly flexible broadband terahertz metamaterial quarter-wave plate. Laser Photonics Rev. 2014, 8, 626–632.
16. Yang, K.; Liu, S.; Arezoomandan, S.; Nahata, A.; Sensale-Rodriguez, B. Graphene-based tunable metamaterial terahertz filters. Appl. Phys. Lett. 2014, 105, 093105.
17. Yao, G.; Ling, F.; Yue, J.; Luo, C.; Ji, J.; Yao, J. Dual-band tunable perfect metamaterial absorber in the THz range. Opt. Express 2016, 24, 1518–1527.
18. Wang, B.-X.; Wang, G.-Z. Temperature tunable metamaterial absorber at THz frequencies. J. Mater. Sci. Mater. Electron. 2017, 28, 8487–8493.
19. Huang, M.; Cheng, Y.; Cheng, Z.; Chen, H.; Mao, X.; Gong, R. Based on graphene tunable dual-band terahertz metamaterial absorber with wide-angle. Opt. Commun. 2018, 415, 194–201.
20. Liu, G.D.; Zhai, X.; Meng, H.Y.; Lin, Q.; Huang, Y.; Zhao, C.J.; Wang, L.L. Dirac semimetals based tunable narrowband absorber at terahertz frequencies. Opt. Express 2018, 26, 11471–11480.
21. Ding, F.; Cui, Y.; Ge, X.; Jin, Y.; He, S. Ultra-broadband microwave metamaterial absorber. Appl. Phys. Lett. 2012, 100, 103506.
22. Wu, Z.; Zhang, Z.L.; Chen, X.Q.; Feng, F.; Zhang, L.; Lv, Y.Y.; He, Y.Y.; Zou, Y.H. Microwave scattering-absorption properties of a lightweight all-dielectric coding metamaterial based on TiO2/CNTs. Opt. Lett. 2020, 45, 555–558.
23. Datta, S.; Mukherjee, S.; Shi, X.D.; Haq, M.; Deng, Y.M.; Udpa, L.; Rothwell, E. Negative index metamaterial lens for subwavelength microwave detection. Sensors 2021, 21, 4782.
24. Xu, J.; Fan, Y.C.; Su, X.P.; Guo, J.; Zhu, J.X.; Fu, Q.H.; Zhang, F.L. Broadband and wide angle microwave absorption with optically transparent metamaterial. Opt. Mater. 2021, 113, 110852.
25. Wang, Y.; Sun, T.; Paudel, T.; Zhang, Y.; Ren, Z.; Kempa, K. Metamaterial-plasmonic absorber structure for high efficiency amorphous silicon solar cells. Nano Lett. 2012, 12, 440–445.
26. Watts, C.M.; Liu, X.; Padilla, W.J. Metamaterial electromagnetic wave absorbers. Adv. Mater. 2012, 24, OP98–OP120.

27. Cong, L.; Cao, W.; Zhang, X.; Tian, Z.; Gu, J.; Singh, R.; Han, J.; Zhang, W. A perfect metamaterial polarization rotator. Appl. Phys. Lett. 2013, 103, 171107.
28. Withayachumnankul, W.; Jaruwongrungsee, K.; Tuantranont, A.; Fumeaux, C.; Abbott, D. Metamaterial-based microfluidic sensor for dielectric characterization. Sens. Actuators A Phys. 2013, 189, 233–237.
29. Yu-Sheng, L.; Chia-Yi, H.; Chengkuo, L. Reconfiguration of resonance characteristics for terahertz U-shape metamaterial using MEMS mechanism. IEEE J. Sel. Top. Quantum Electron. 2015, 21, 93–99.
30. Lochbaum, A.; Fedoryshyn, Y.; Dorodnyy, A.; Koch, U.; Hafner, C.; Leuthold, J. On-chip narrowband thermal emitter for Mid-IR optical gas sensing. ACS Photonics 2017, 4, 1371–1380.
31. Appavoo, K.; Haglund, R.F. Detecting nanoscale size dependence in VO2 phase transition using a split-ring resonator metamaterial. Nano Lett. 2011, 11, 1025–1031.
32. Wang, H.; Yang, Y.; Wang, L. Switchable wavelength-selective and diffuse metamaterial absorber/emitter with a phase transition spacer layer. Appl. Phys. Lett. 2014, 105, 071907.
33. Lei, L.; Lou, F.; Tao, K.Y.; Huang, H.X.; Cheng, X.; Xu, P. Tunable and scalable broadband metamaterial absorber involving VO2-based phase transition. Photonics Res. 2019, 7, 734–741.
34. Chen, P.-Y.; Alu, A. Terahertz metamaterial devices based on graphene nanostructures. IEEE Trans. Terahertz Sci. Technol. 2013, 3, 748–756.
35. Zhang, Y.; Li, T.; Chen, Q.; Zhang, H.; O'Hara, J.F.; Abele, E.; Taylor, A.J.; Chen, H.T.; Azad, A.K. Independently tunable dual-band perfect absorber based on graphene at mid-infrared frequencies. Sci. Rep. 2015, 5, 18463.
36. Li, H.; Wang, L.; Zhai, X. Tunable graphene-based mid-infrared plasmonic wide-angle narrowband perfect absorber. Sci. Rep. 2016, 6, 36651.
37. Zhang, J.; Wang, G.; Zhang, B.; He, T.; He, Y.; Shen, J. Photo-excited broadband tunable terahertz metamaterial absorber. Opt. Mater. 2016, 54, 32–36.
38. Shrekenhamer, D.; Chen, W.C.; Padilla, W.J. Liquid crystal tunable metamaterial absorber. Phys. Rev. Lett. 2013, 110, 177403.
39. Ou, J.Y.; Plum, E.; Zhang, J.; Zheludev, N.I. Giant nonlinearity of an optically reconfigurable plasmonic metamaterial. Adv. Mater. 2016, 28, 729–733.
40. Kim, J.; Jeong, H.; Lim, S. Mechanically actuated frequency reconfigurable metamaterial absorber. Sens. Actuators A Phys. 2019, 299, 111619.
41. Zhu, W.M.; Liu, A.Q.; Zhang, W.; Tao, J.F.; Bourouina, T.; Teng, J.H.; Zhang, X.H.; Wu, Q.Y.; Tanoto, H.; Guo, H.C.; et al. Polarization dependent state to polarization independent state

change in THz metamaterials. Appl. Phys. Lett. 2011, 99.

42. Zhu, W.M.; Liu, A.Q.; Bourouina, T.; Tsai, D.P.; Teng, J.H.; Zhang, X.H.; Lo, G.Q.; Kwong, D.L.; Zheludev, N.I. Microelectromechanical Maltese-cross metamaterial with tunable terahertz anisotropy. Nat. Commun. 2012, 3, 1274.
43. Liu, X.; Padilla, W.J. Dynamic manipulation of infrared radiation with MEMS metamaterials. Adv. Opt. Mater. 2013, 1, 559–562.
44. Ho, C.P.; Pitchappa, P.; Lin, Y.-S.; Huang, C.-Y.; Kropelnicki, P.; Lee, C. Electrothermally actuated microelectromechanical systems based omega-ring terahertz metamaterial with polarization dependent characteristics. Appl. Phys. Lett. 2014, 104, 161104.
45. Pitchappa, P.; Ho, C.P.; Dhakar, L.; Lee, C. Microelectromechanically reconfigurable interpixelated metamaterial for independent tuning of multiple resonances at terahertz spectral region. Optica 2015, 2, 571–578.
46. Pitchappa, P.; Ho, C.P.; Cong, L.; Singh, R.; Singh, N.; Lee, C. Reconfigurable digital metamaterial for dynamic switching of terahertz anisotropy. Adv. Opt. Mater. 2016, 4, 391–398.
47. Liu, X.; Padilla, W.J. Reconfigurable room temperature metamaterial infrared emitter. Optica 2017, 4, 430–433.
48. Zhao, X.; Schalch, J.; Zhang, J.; Seren, H.R.; Duan, G.; Averitt, R.D.; Zhang, X. Electromechanically tunable metasurface transmission waveplate at terahertz frequencies. Optica 2018, 5, 303–310.
49. Xu, Z.; Lin, Y.S. A stretchable terahertz parabolic-shaped metamaterial. Adv. Opt. Mater. 2019, 7, 1900379.
50. Mo, Y.; Zhong, J.; Lin, Y.-S. Tunable chevron-shaped infrared metamaterial. Mater. Lett. 2020, 263, 127291.
51. Xu, R.; Lin, Y.S. Flexible and controllable metadevice using self-assembly MEMS actuator. Nano Lett. 2021, 21, 3205–3210.
52. Ou, J.Y.; Plum, E.; Jiang, L.; Zheludev, N.I. Reconfigurable photonic metamaterials. Nano Lett. 2011, 11, 2142–2144.
53. Pitchappa, P.; Ho, C.P.; Kropelnicki, P.; Singh, N.; Kwong, D.L.; Lee, C. Micro-electro-mechanically switchable near infrared complementary metamaterial absorber. Appl. Phys. Lett. 2014, 104, 201114.
54. Ivzhenko, L.; Odarenko, E.; Tarapov, S.I. Mechanically tunable wire medium metamaterial in the millimeter wave band. Prog. Electromagn. Res. 2016, 64, 93–98.

55. Liu, J.J.; Hong, Z. Mechanically tunable dual frequency THz metamaterial filter. Opt. Commun. 2018, 426, 598–601.
56. Morris, C.; Bekker, L.; Spadaccini, C.; Haberman, M.; Seepersad, C. Tunable mechanical metamaterial with constrained negative stiffness for improved quasi-static and dynamic energy dissipation. Adv. Eng. Mater. 2019, 21, 1900163.
57. Chen, F.Q.; Liu, X.J.; Tian, Y.P.; Zheng, Y. Mechanically stretchable metamaterial with tunable mid-infrared optical properties. Opt. Express 2021, 29, 37368–37375.
58. Tao, H.; Strikwerda, A.C.; Fan, K.; Padilla, W.J.; Zhang, X.; Averitt, R.D. Reconfigurable terahertz metamaterials. Phys. Rev. Lett. 2009, 103, 147401.
59. Pitchappa, P.; Manjappa, M.; Krishnamoorthy, H.N.S.; Chang, Y.; Lee, C.; Singh, R. Bidirectional reconfiguration and thermal tuning of microcantilever metamaterial device operating from 77 K to 400 K. Appl. Phys. Lett. 2017, 111, 261101.
60. Zhong, J.; Xu, X.; Lin, Y.-S. Tunable terahertz metamaterial with electromagnetically induced transparency characteristic for sensing application. Nanomaterials 2021, 11, 2175.
61. Yang, J.; Lin, Y.-S. Design of tunable terahertz metamaterial sensor with single- and dual-resonance characteristic. Nanomaterials 2021, 11, 2212.
62. Xu, R.; Xu, X.; Yang, B.-R.; Gui, X.; Qin, Z.; Lin, Y.-S. Actively logical modulation of MEMS-based terahertz metamaterial. Photonics Res. 2021, 9.
63. Li, X.; Yang, T.; Zhu, W.; Li, X. Continuously tunable terahertz metamaterial employing a thermal actuator. Microsyst. Technol. 2012, 19, 1145–1151.
64. Lalas, A.; Kantartzis, N.; Tsiboukis, T. Programmable terahertz metamaterials through V-beam electrothermal devices. Appl. Phys. A 2014, 117, 433–438.
65. Lalas, A.X.; Kantartzis, N.V.; Tsiboukis, T.D. Reconfigurable metamaterial components exploiting two-hot-arm electrothermal actuators. Microsyst. Technol. 2015, 21, 2097–2107.
66. Lin, Y.-S.; Qian, Y.; Ma, F.; Liu, Z.; Kropelnicki, P.; Lee, C. Development of stress-induced curved actuators for a tunable THz filter based on double split-ring resonators. Appl. Phys. Lett. 2013, 102, 111908.
67. Liu, M.; Susli, M.; Silva, D.; Putrino, G.; Kala, H.; Fan, S.; Cole, M.; Faraone, L.; Wallace, V.P.; Padilla, W.J.; et al. Ultrathin tunable terahertz absorber based on MEMS-driven metamaterial. Microsyst. Nanoeng. 2017, 3, 17033.
68. Manjappa, M.; Pitchappa, P.; Singh, N.; Wang, N.; Zheludev, N.I.; Lee, C.; Singh, R. Reconfigurable MEMS Fano metasurfaces with multiple-input-output states for logic operations at terahertz frequencies. Nat. Commun. 2018, 9, 4056.

69. Lin, Y.S.; Ma, F.; Lee, C. Three-dimensional movable metamaterial using electric split-ring resonators. Opt. Lett. 2013, 38, 3126–3128.
70. Pitchappa, P.; Ho, C.P.; Dhakar, L.; Qian, Y.; Singh, N.; Lee, C. Periodic array of subwavelength MEMS cantilevers for dynamic manipulation of terahertz waves. J. Microelectromech. Syst. 2015, 24, 525–527.
71. Zhengli, H.; Kohno, K.; Fujita, H.; Hirakawa, K.; Toshiyoshi, H. Tunable terahertz filter and modulator based on electrostatic MEMS reconfigurable SRR array. IEEE J. Sel. Top. Quantum Electron. 2015, 21, 114–122.
72. Shih, K.; Pitchappa, P.; Manjappa, M.; Ho, C.P.; Singh, R.; Yang, B.; Singh, N.; Lee, C. Active MEMS metamaterials for THz bandwidth control. Appl. Phys. Lett. 2017, 110, 161108.
73. Pitchappa, P.; Ho, C.P.; Qian, Y.; Dhakar, L.; Singh, N.; Lee, C. Microelectromechanically tunable multiband metamaterial with preserved isotropy. Sci. Rep. 2015, 5, 11678.
74. Pitchappa, P.; Manjappa, M.; Ho, C.P.; Qian, Y.; Singh, R.; Singh, N.; Lee, C. Active control of near-field coupling in conductively coupled microelectromechanical system metamaterial devices. Appl. Phys. Lett. 2016, 108, 111102.
75. Ma, F.; Qian, Y.; Lin, Y.-S.; Liu, H.; Zhang, X.; Liu, Z.; Ming-Lin Tsai, J.; Lee, C. Polarization-sensitive microelectromechanical systems based tunable terahertz metamaterials using three dimensional electric split-ring resonator arrays. Appl. Phys. Lett. 2013, 102, 161912.
76. Lin, Y.-S.; Lee, C. Tuning characteristics of mirrorlike T-shape terahertz metamaterial using out-of-plane actuated cantilevers. Appl. Phys. Lett. 2014, 104, 251914.
77. Schalch, J.; Duan, G.W.; Zhao, X.G.; Zhang, X.; Averitt, R.D. Terahertz metamaterial perfect absorber with continuously tunable air spacer layer. Appl. Phys. Lett. 2018, 113, 061113.
78. Liu, S.; Zhang, L.; Bai, G.D.; Cui, T.J. Flexible controls of broadband electromagnetic wavefronts with a mechanically programmable metamaterial. Sci. Rep. 2019, 9, 1809.
79. Wang, J.; Tian, H.; Wang, G.C.; Li, S.; Guo, W.P.; Xing, J.; Wang, Y.; Li, L.; Zhou, Z.X. Mechanical control of terahertz plasmon-induced transparency in single/double-layer stretchable metamaterial. J. Phys. D Appl. Phys. 2021, 54, 035101.
80. Fu, Y.H.; Liu, A.Q.; Zhu, W.M.; Zhang, X.M.; Tsai, D.P.; Zhang, J.B.; Mei, T.; Tao, J.F.; Guo, H.C.; Zhang, X.H.; et al. A micromachined reconfigurable metamaterial via reconfiguration of asymmetric split-ring resonators. Adv. Funct. Mater. 2011, 21, 3589–3594.
81. Zhu, W.M.; Liu, A.Q.; Zhang, X.M.; Tsai, D.P.; Bourouina, T.; Teng, J.H.; Zhang, X.H.; Guo, H.C.; Tanoto, H.; Mei, T.; et al. Switchable magnetic metamaterials using micromachining processes. Adv. Mater. 2011, 23, 1792–1796.

82. Wu, Z.; Wei Ming, Z.; Hong, C.; Tsai, M.L.J.; Guo-Qiang, L.; Din Ping, T.; Tanoto, H.; Jing-Hua, T.; Xin-Hai, Z.; Dim-Lee, K.; et al. Resonance switchable metamaterials using MEMS fabrications. IEEE J. Sel. Top. Quantum Electron. 2013, 19, 4700306.
83. Zhao, X.; Fan, K.; Zhang, J.; Keiser, G.R.; Duan, G.; Averitt, R.D.; Zhang, X. Voltage-tunable dual-layer terahertz metamaterials. Microsyst. Nanoeng. 2016, 2, 16025.
84. Huang, Y.; Nakamura, K.; Takida, Y.; Minamide, H.; Hane, K.; Kanamori, Y. Actively tunable THz filter based on an electromagnetically induced transparency analog hybridized with a MEMS metamaterial. Sci. Rep. 2020, 10, 20807.
85. Zhang, M.; Zhang, W.; Liu, A.Q.; Li, F.C.; Lan, C.F. Tunable polarization conversion and rotation based on a reconfigurable metasurface. Sci. Rep. 2017, 7, 12068.
86. Wen, Y.; Liang, Z.; Lin, Y.-S.; Chen, C.-H. Active modulation of polarization-sensitive infrared metamaterial. Opt. Commun. 2020, 463, 125489.
87. Xu, T.; Lin, Y.-S. Tunable terahertz metamaterial using an electric split-ring resonator with polarization-sensitive characteristic. Appl. Sci. 2020, 10, 4660.
88. Xu, T.; Xu, R.; Lin, Y.-S. Tunable terahertz metamaterial using electrostatically electric split-ring resonator. Results Phys. 2020, 19, 103638.
89. Xu, T.; Xu, X.; Lin, Y.-S. Tunable terahertz free spectra range using electric split-ring metamaterial. J. Microelectromech. Syst. 2021, 30, 309–314.
90. Zheludev, N.I.; Plum, E. Reconfigurable nanomechanical photonic metamaterials. Nat. Nanotechnol. 2016, 11, 16–22.
91. Kang, L.; Zhao, Q.; Zhao, H.J.; Zhou, J. Ferrite-based magnetically tunable left-handed metamaterial composed of SRRs and wires. Opt. Express 2008, 16, 17269–17275.
92. Cho, I.-J.; Yoon, E. A low-voltage three-axis electromagnetically actuated micromirror for fine alignment among optical devices. J. Micromech. Microeng. 2009, 19, 085007.
93. Ozbey, B.; Aktas, O. Continuously tunable terahertz metamaterial employing magnetically actuated cantilevers. Opt. Express 2011, 19, 5741–5752.
94. Khodasevych, I.E.; Shah, C.M.; Rowe, W.S.T.; Mitchell, A. Flexible fishnet metamaterial on PDMS substrate for THz frequencies. In Proceedings of the 2010 Conference on Optoelectronic and Microelectronic Materials and Devices, Canberra, Australia, 12–15 December 2010; pp. 25–26.
95. Ling, K.; Kim, K.; Lim, S. Flexible liquid metal-filled metamaterial absorber on polydimethylsiloxane (PDMS). Opt. Express 2015, 23, 21375–21383.
96. Malek, S.C.; Ee, H.S.; Agarwal, R. Strain multiplexed metasurface holograms on a stretchable substrate. Nano Lett. 2017, 17, 3641–3645.

97. Li, J.; Shah, C.M.; Withayachumnankul, W.; Ung, B.S.Y.; Mitchell, A.; Sriram, S.; Bhaskaran, M.; Chang, S.; Abbott, D. Mechanically tunable terahertz metamaterials. Appl. Phys. Lett. 2013, 102, 012110.
98. Zhang, F.; Feng, S.; Qiu, K.; Liu, Z.; Fan, Y.; Zhang, W.; Zhao, Q.; Zhou, J. Mechanically stretchable and tunable metamaterial absorber. Appl. Phys. Lett. 2015, 106, 091907.
99. Kim, K.; Lee, D.; Eom, S.; Lim, S. Stretchable metamaterial absorber using liquid metal-filled polydimethylsiloxane (PDMS). Sensors 2016, 16, 521.
100. Ee, H.S.; Agarwal, R. Tunable metasurface and flat optical zoom lens on a stretchable substrate. Nano Lett. 2016, 16, 2818–2823.
101. Xu, R.; Luo, J.; Sha, J.; Zhong, J.; Xu, Z.; Tong, Y.; Lin, Y.-S. Stretchable IR metamaterial with ultra-narrowband perfect absorption. Appl. Phys. Lett. 2018, 113, 101907.
102. Zhang, H.; Feng, L.; Liang, Y.Z.; Xu, T. An ultra-flexible plasmonic metamaterial film for efficient omnidirectional and broadband optical absorption. Nanoscale 2019, 11, 437–443.
103. Gao, Z.Q.; Xu, C.L.; Tian, X.X.; Wang, J.F.; Tian, C.H.; Yang, B.Y.; Qu, S.B.; Fan, Q. Ultra-wideband flexible transparent metamaterial with wide-angle microwave absorption and low infrared emissivity. Opt. Express 2021, 29, 22108–22116.